

Caspase-4 activation by a bacterial surface protein is mediated by cathepsin G in human gingival fibroblasts

Hye-Kyoung Jun^{1,4}, Young-Jung Jung^{1,5}, Suk Ji², Sun-Jin An¹ and Bong-Kyu Choi^{*,1,3}

Caspase-4 is an inflammatory caspase; however, its mechanism of activation is poorly understood. In this study, we demonstrate that Td92, a surface protein of the periodontal pathogen *Treponema denticola* and a homolog of the *Treponema pallidum* surface protein Tp92, activates caspase-4 and induces pyroptosis in primary cultured human gingival fibroblasts (HGFs) via cathepsin G activation. Cathepsin G inhibition or siRNA knockdown of cathepsin G inhibited Td92-induced caspase-4 activation and cell death. Td92-induced cell death was significantly inhibited by siRNA knockdown of gasdermin D. Td92 treatment resulted in the binding of cathepsin G to caspase-4 and the coaggregation of these two molecules. In addition, Td92 induced IL-1 α expression and secretion, and this was inhibited by caspase-4 knockdown. Cytochalasin D did not block Td92-induced caspase-4 activation, suggesting that Td92 internalization is not required for caspase-4 activation. Our results demonstrate that cathepsin G is directly engaged in caspase-4 activation by a bacterial ligand, which is responsible for cell death and IL-1 α secretion in HGFs.

Cell Death and Differentiation (2018) 25, 380–391; doi:10.1038/cdd.2017.167; published online 27 October 2017

Caspases are aspartate-specific cysteine proteases involved in programmed cell death and inflammation. Of the inflammatory caspases (caspase-1, -4, -5 and -12 in humans), caspase-1 is the best characterized.¹ The canonical inflammasome activates caspase-1, which can process pro-IL-1 β and pro-IL-18 into their active and secreted forms.² Caspase-1 and caspase-11 have been shown to cleave gasdermin D, generating an N-terminal cleavage product that forms pores in the cell membrane by oligomerization, resulting in cell death.^{3–6}

Studies of the role of human caspase-4, the functional ortholog of murine caspase-11, have focused on endoplasmic reticulum (ER) stress-induced apoptosis.^{7–9} However, recent studies have also demonstrated its role in canonical and noncanonical inflammasome activation and inflammatory cell death.^{10–13} Caspase-4, which is located in the same locus as the caspase-1, -5 and -12 genes, is involved in NLRP3 inflammasome-mediated caspase-1 activation in skin keratinocytes stimulated with UVB, resulting in activation of pro-IL-1 β .¹⁴ Caspase-4 has a major role in proinflammatory cell death in keratinocytes via the TLR3 ligand¹⁵ and in epithelial cells infected with *Shigella*.¹⁶ Activation of caspase-4 by *Legionella pneumophila* is independent of caspase-1 and IL-1 β maturation but induces cell death and IL-1 α secretion in human macrophages.¹⁰ Caspase-4 activated by intracellular LPS controls both IL-1 α and IL-1 β secretion, as well as cell death. Intracellular LPS interacts directly with caspase-4, or its murine ortholog caspase-11, followed by activation of these caspases, which results in caspase-1-independent pyroptosis.¹³

Cathepsin G is a serine protease belonging to the chymotrypsin superfamily. Human cathepsin G is synthesized as a 255-aa prepropeptide. The 18-aa signal peptide and the following dipeptide (Gly19 and Glu20) are removed for activation.¹⁷ Cathepsin G has antimicrobial activity and is involved in chemotaxis, apoptosis, the immune response and inflammation, hydrolysis of extracellular matrix proteins and platelet activation.^{18–20}

Periodontitis is a type of chronic inflammation induced by multiple pathogenic species present in subgingival pockets, leading to tooth loss. Periodontal pathogens are in contact with the sulcular epithelium and several pathogens penetrate deep into the gingival connective tissue.²¹ Human gingival fibroblasts (HGFs) are the most abundant cells in gingival connective tissue and they participate actively in the inflammatory response to bacterial infection. Proinflammatory cell death induced by caspase-1 and caspase-4 functions as a host-defense mechanism by eliminating invading pathogens and activating the innate immune system in the early phase of infection. However, cell death can facilitate the dissemination of pathogens into deep sites to promote infection. Recently, we reported that Td92, a surface protein of the major periodontopathogen *T. denticola*, interacts with integrin $\alpha 5 \beta 1$, activates caspase-1 via the NLRP3 inflammasome and induces pyroptosis in macrophages.²² Td92-homologous proteins are present on the surface of several species of oral *Treponema* and of *T. pallidum*, the causative agent of syphilis.^{23,24}

In this study, we show that Td92 activates caspase-4 independently of caspase-1 in primary cultured HGFs via

¹Department of Oral Microbiology and Immunology, School of Dentistry, Seoul National University, 101 Daehak-ro, Jongno-gu, Seoul 03080, Republic of Korea;

²Department of Periodontology, Ajou University Hospital, 164 Worldcup-ro, Yeongtong-gu, Suwon 16499, Republic of Korea and ³Dental Research Institute, School of Dentistry, Seoul National University, 101 Daehak-ro, Jongno-gu, Seoul 03080, Republic of Korea

*Corresponding author: B-K Choi, Department of Oral Microbiology and Immunology, School of Dentistry, Seoul National University, 101 Daehak-ro, Jongno-gu, Seoul 03080, Republic of Korea. Tel: +82 2 740 8640; Fax: +82 2 743 0311; E-mail: bongchoi@snu.ac.kr

⁴Current address: Institute of Bone Science, OSSTEM IMPLANT Co., Ltd, Seoul 02861, Republic of Korea

⁵Current address: Department of Oral Immunology and Infectious Diseases, University of Louisville School of Dentistry, Louisville, KY 402, USA

Received 24.1.17; revised 22.8.17; accepted 08.9.17; Edited by RA Knight; published online 27.10.17

cathepsin G activation. Td92-activated caspase-4 induces pyroptotic cell death and IL-1 α secretion. Interaction of Td92 with integrin $\alpha 5\beta 1$ without internalization into cells results in caspase-4 activation. Our elucidation of the role of cathepsin G in caspase-4 activation by the bacterial surface protein Td92 enhances the understanding of the role of caspase-4 in the innate immune response and cell death.

Results

Td92 activates caspase-4. In a previous study, we demonstrated that the *T. denticola* surface protein Td92 activates caspase-1 and pyroptosis in macrophages via NLRP3 inflammasome activation by interaction with integrin $\alpha 5\beta 1$.²² Recent reports of caspase-4 involvement in inflammasome activation and cell death prompted us to analyze the role of Td92 in caspase-4 activation in different cell types. Caspase-4 is expressed in various tissues and is composed of a prodomain (p22) and two small domains (p20 and p10) that are cleaved upon activation, similar to caspase-1. Activation of caspase-4 was detected by the appearance of cleaved caspase-4 products (20 kDa fragments). When THP-1 macrophages were treated with Td92, the activated form of caspase-4 was detected in culture supernatants (Figure 1a). Caspase-4 activation was also detected in cells treated with Pam3CSK4, a ligand of the NLRP7 inflammasome.²⁵ Td-B (the C-terminal half of Td92 (Jun *et al.*²²)) did not activate caspase-4. Td-G (the N-terminal half of Td92), which could activate caspase-1 in THP-1 cells,²² also activated caspase-4 (Figure 1a). The dose-dependent

release of active caspase-4 by Td92 was observed in PBMC-derived macrophages as well as in THP-1 cells (Figure 1b).

Next, we tested the ability of Td92 to induce caspase activation in primary cultured HGFs. Td92 induced caspase-4 activation in HGFs (Figure 1c). In contrast to caspase-1 activation in THP-1 cells and PBMC-derived macrophages,²² Td92 did not induce caspase-1 activation or IL-1 β secretion in HGFs. Interestingly, the synthetic peptide Pam3CSK4, which also induced caspase-4 activation in THP-1 cells, did not induce caspase-4 activation in HGFs. These results indicate that caspase-1 and caspase-4 are regulated differently depending on cell type and ligand. Td92-activated caspase-4 was inhibited by a neutralizing antibody to integrin $\alpha 5\beta 1$, but not by cytochalasin D (Supplementary Figure 1), as previously shown for Td92-induced caspase-1 activation in macrophages.²² To elucidate the underlying mechanisms of caspase-4 activation, we used HGFs for further experiments. Similar to caspase-1, active caspase-4 was rarely detected in cell lysates as its secretion occurred quickly, which may minimize intracellular proteolytic activity.²

Type I interferon (IFN) signaling induces the expression and activation of murine caspase-11, the functional ortholog of human caspase-4.²⁶ To test whether IFN signaling is involved in Td92-induced caspase-4 expression and activation, HGFs were treated with Td92 and mRNA expression of IFN- β was analyzed. As shown in Supplementary Figure 2a, Td92 significantly induced IFN- β mRNA expression as early as 3 h after treatment. However, neutralizing IFN- β antibody did not inhibit Td92-induced caspase-4 mRNA expression and activation up to 16 h later (Supplementary Figures 2b and c).

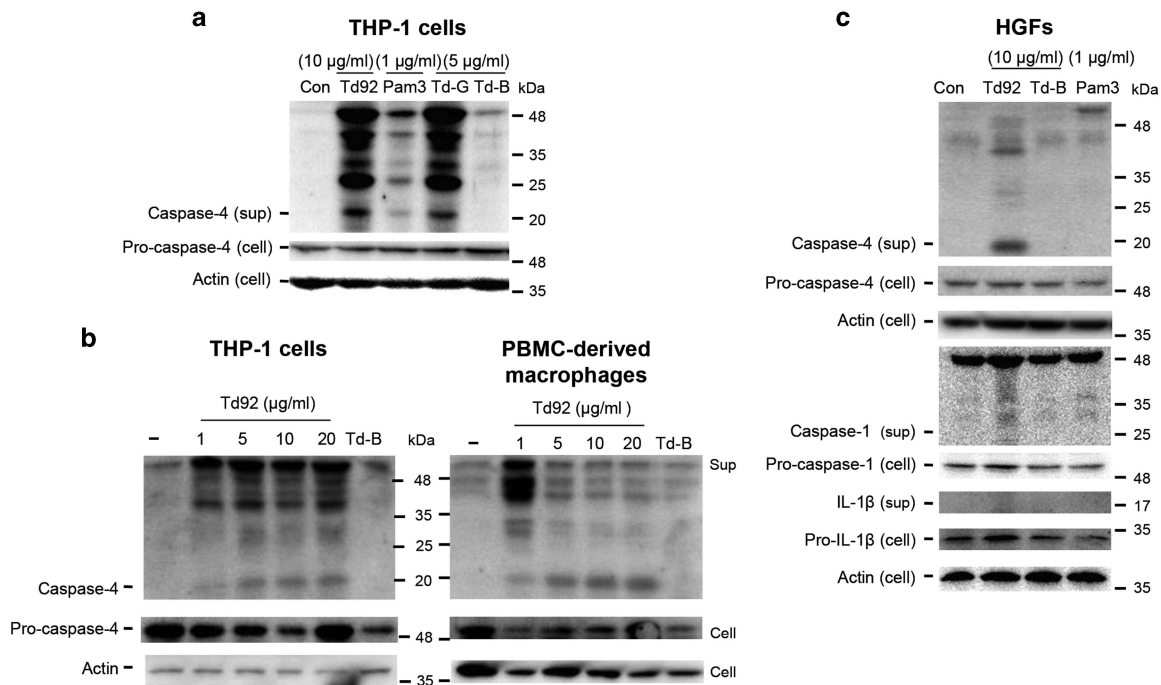


Figure 1 Td92 induces caspase-4 activation. THP-1 cells (a and b), PBMC-derived macrophages (b) and HGFs (c) were treated with Td92, Td-G, Td-B or Pam3CSK4 (Pam3) for 6 h. Caspase-1, caspase-4, and IL-1 β in the culture supernatants and pro-caspase-1, pro-caspase-4, pro-IL-1 β , and actin in cell lysates were detected by western blotting

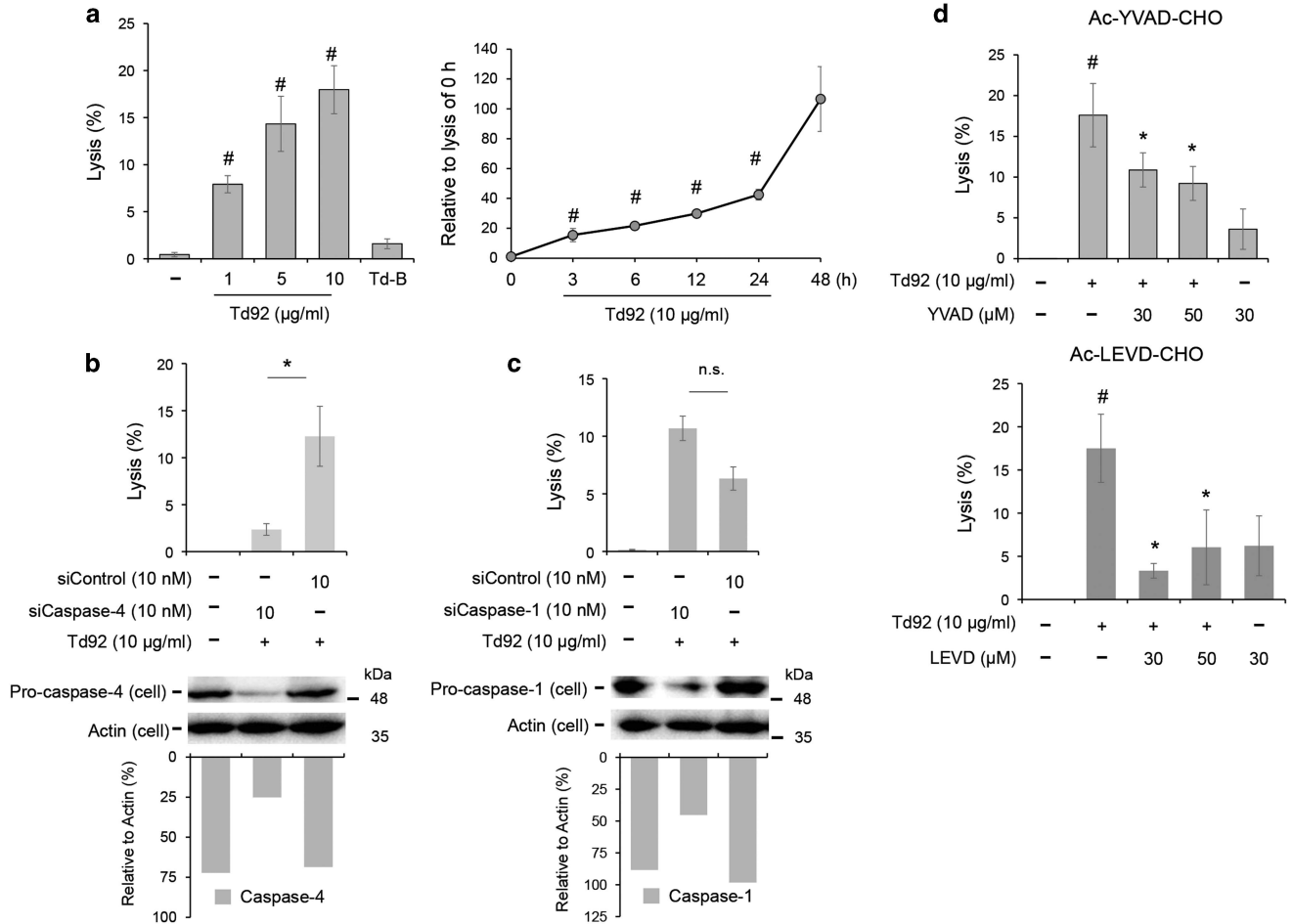


Figure 2 Caspase-4 is responsible for cell death in HGFs. (a) HGFs were stimulated with various doses of Td92 for 6 h or 10 μg/ml of Td92 for various incubation times. Cell culture supernatants were evaluated for the release of the cytoplasmic enzyme LDH. #*P* < 0.01 compared to non-treated control. HGFs were transfected with control siRNA or siRNA specific for caspase-4 (b) or caspase-1 (c) for 24 h. Transfection efficiency was confirmed by western blotting. siRNA-transfected cells were treated with Td92 for 6 h and cell culture supernatants were evaluated for LDH level. **P* < 0.01 compared with control siRNA-transfected cells. Densitometric analysis of expression of caspase-4 (b) and caspase-1 (c) relative to actin is shown. (d) HGFs were pretreated with Ac-YVAD-CHO or Ac-LEVD-CHO before treatment with Td92 (10 μg/ml) for 6 h. Cell culture supernatants were evaluated for LDH level. #*P* < 0.01 compared to non-treated control and **P* < 0.05 compared with Td92-stimulated cells. Data are shown as the means ± S.D. of three independent experiments performed in triplicate

These results indicate that type I IFN signaling is not involved in Td92-induced caspase-4 activation.

Td92-activated caspase-4 induces cell death. We tested whether Td92-activated caspase-4 induces cell death of HGFs by measuring LDH release. Td92 induced dose- and time-dependent LDH release (Figure 2a), and siRNA-mediated caspase-4 knockdown significantly reduced the LDH release induced by Td92 (Figure 2b). In contrast, caspase-1 knockdown did not affect Td92-induced LDH release in HGFs (Figure 2c). Caspase-4 and caspase-1 RNA interference was confirmed by real-time qPCR (data not shown) and western blotting (Figure 2b and c). We also used caspase inhibitors to confirm the role of caspase-4 in Td92-induced cell death. The caspase inhibitors Ac-YVAD-CHO (a caspase-1/4 inhibitor) and Ac-LEVD-CHO (a caspase-4/5 inhibitor) significantly inhibited LDH release (Figure 2d).

These results suggest that caspase-4 is responsible for cell death in HGFs treated with Td92.

ER stress is involved in caspase-4 activation and apoptosis.²⁷ To clarify the role of ER stress in Td92-induced caspase-4 activation, the expression of ER stress markers, including glucose-regulated protein 78 kDa (GRP78) and CCAAT/enhancer-binding protein homologous protein (CHOP), was evaluated. Td92 did not induce mRNA expression of GRP78 or CHOP for up to 12 h, whereas the ER stress inducer thapsigargin significantly increased mRNA expression of GRP78 and CHOP (Supplementary Figure 3).

To further confirm that Td92 induced pyroptosis but not apoptosis, HGFs were treated with Td92 and stained with propidium iodide (PI) and Annexin V. We scored PI⁺/Annexin V⁻ cells as positive for pyroptosis and PI⁻/Annexin V⁺ as positive for apoptosis. Flow cytometric analysis showed that Td92 significantly increased the proportion of PI⁺/Annexin V⁻ cells but not PI⁻/Annexin V⁺ cells in HGFs after 16 h

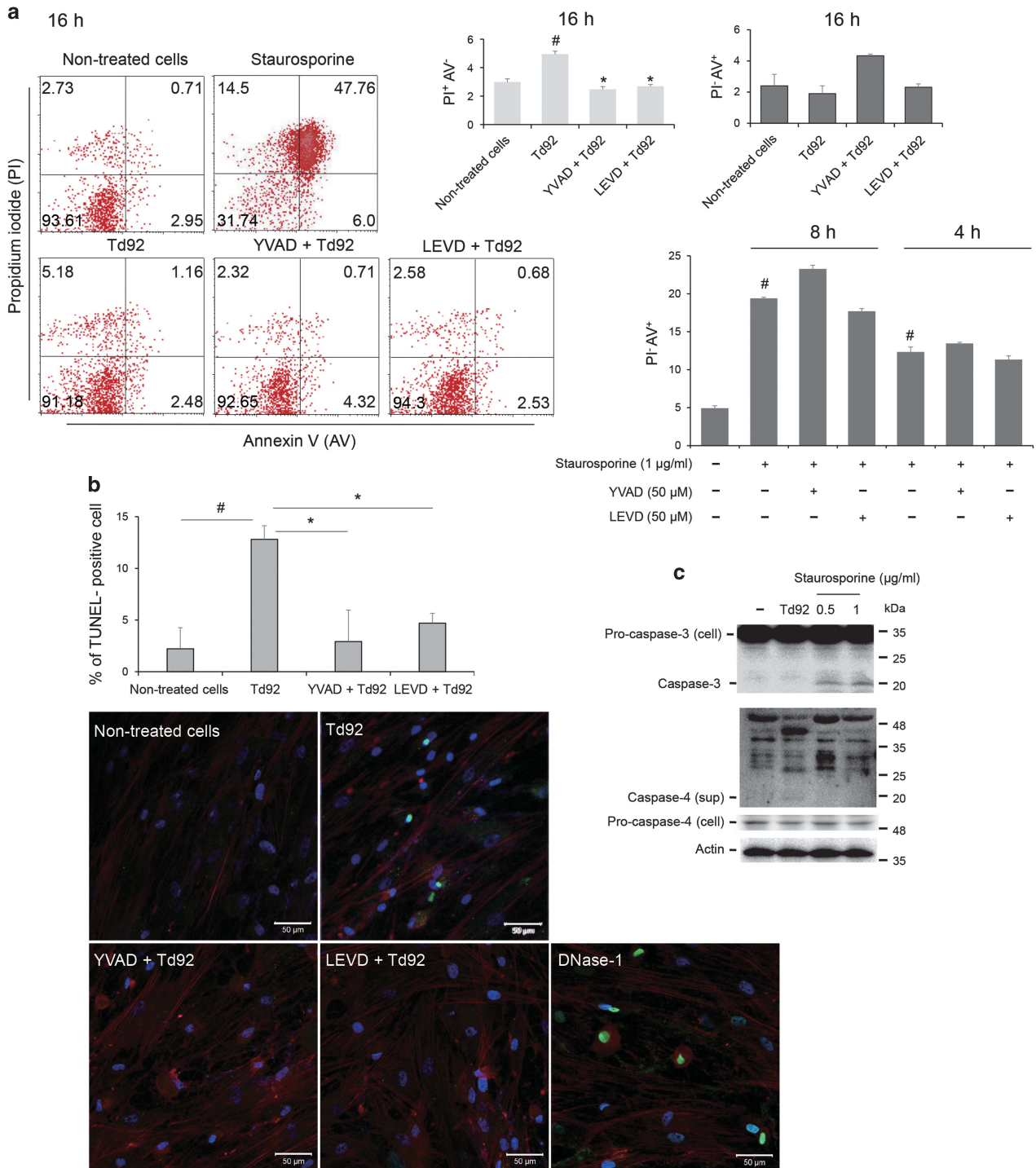


Figure 3 Td92 induces PI uptake and DNA fragmentation. (a) HGFs were treated with Td92 (10 μg/ml) or staurosporine (1 μg/ml) for the indicated times in the presence or absence of Ac-YVAD-CHO (YVAD, 50 μM) or Ac-LEVD-CHO (LEVD, 50 μM) and stained with PI and Annexin V followed by flow cytometric analysis. (b) HGFs were pretreated with Ac-YVAD-CHO (YVAD, 50 μM) or Ac-LEVD-CHO (LEVD, 50 μM) for 30 min before treatment with Td92 (10 μg/ml) for 16 h. Cells were subjected to TUNEL assay and observed by confocal laser scanning microscopy. Images of 10 microscopic fields per well were taken at ×200 magnification and the percentage of TUNEL-positive cells was calculated using NIH ImageJ software. At least 500 cells were counted for each experimental condition. Scale bars represent 50 μm. Data are shown as the means ± S.D. of three independent experiments performed in triplicate. #*P* < 0.01 compared with non-treated controls and **P* < 0.05 compared with Td92-stimulated cells. (c) HGFs were treated with Td92 (10 μg/ml) or staurosporine at the indicated dose for 6 h. Caspase-4 in the culture supernatants and caspase-3, pro-caspase-3, pro-caspase-4 and actin in the cell lysates were detected by western blotting

treatments (Figure 3a), whereas neither PI⁺/Annexin V⁻ nor PI⁻/Annexin V⁺ cells were observed after 4- and 8 h treatments (Supplementary Figure 4). Staurosporine, an apoptosis inducer, significantly increased the proportion of PI⁻/Annexin V⁺ cells at 4- and 8 h of incubation. In addition, the proportion of Td92-induced PI⁺/Annexin V⁻ HGFs was significantly decreased by pretreatment with Ac-YVAD-CHO or Ac-LEVD-CHO, whereas staurosporine-induced PI⁻/Annexin V⁺ cells were not affected by these inhibitors. Furthermore, TdT-mediated dUTP nick end-labeling (TUNEL) assay showed that Td92 treatment resulted in nuclear fragmentation (Figure 3b), which was inhibited by Ac-YVAD-CHO or Ac-LEVD-CHO treatment. Td92 treatment did not induce activation of caspase-3, one of the key executors of apoptosis (Figure 3c). Recently, inflammatory caspases have been reported to cleave gasdermin D into a 30 kDa N-terminal and a 22 kDa C-terminal fragment, whereby gasdermin N domains induce pyroptosis by forming oligomeric pores in the cell membrane.^{4-6,28} To determine whether Td92-induced cell death is dependent on gasdermin D, we performed genetic knockdown of gasdermin D using siRNA technology. siRNA knockdown of gasdermin D significantly inhibited cell death induced by Td92 in HGFs (Supplementary Figure 5). These results confirm that Td92-induced caspase-4 activation results in pyroptosis, not ER stress-induced apoptosis.

Td92-induced caspase-4 activation is inhibited by serine protease inhibitors. Bromoenol lactone (BEL) is a serine protease inhibitor. It inhibits the induction of caspase-1 activation and IL-1 β secretion by ATP in LPS-primed macrophages, which activates the NLRP3 inflammasome, and by *Salmonella* infection, which activates the NLRC4 inflammasome.²⁹ In our previous report, Bay 11-7082, an NF- κ B inhibitor that inhibits I κ B α phosphorylation, inhibited Td92-induced caspase-1 activation and IL-1 β secretion, as well as pro-IL-1 β expression, in THP-1 cells.²² Thus, we tested the effect of serine protease inhibitors (BEL and tosyl phenylalanyl chloromethyl ketone (TPCK)) and Bay 11-7082 on Td92-induced caspase-4 activation in HGFs. Pretreatment with serine protease inhibitors reduced caspase-4 activation, whereas Bay 11-7082 did not inhibit caspase-4 activation in HGFs (Figure 4a). Bay 11-7082 and the serine protease inhibitors affected cell death according to their modes of inhibition of caspase-4 activation (Figure 4b). These results suggest that serine proteases have an important role in caspase-4 activation and cell death in HGFs. We also examined whether Bay 11-7082 and serine protease inhibitors affect the expression of caspase-4 mRNA. Td92 significantly induced caspase-4 mRNA expression in HGFs as early as 3 h after stimulation, but the inhibitors did not affect Td92-induced caspase-4 mRNA expression (Supplementary Figure 6), indicating that serine protease inhibitors target caspase-4 activation but not caspase-4 expression.

Td92 activates cathepsin G, which in turn activates caspase-4. Cathepsin G, a serine protease, has been reported to cleave recombinant pro-caspase-7 into a maximally activated form³⁰ and promote caspase-3 activation in cultured rat cardiomyocytes.³¹ As Td92-induced caspase-4

activation was inhibited by serine protease inhibitors, we investigated whether cathepsin G was involved in Td92-induced caspase-4 activation. Human cathepsin G is synthesized as a prepropeptide that is cleaved to yield the active form (28 kDa). Td92 induced the enzymatic activity of cathepsin G in a time- and dose-dependent manner in HGFs (Figure 5a). In non-treated cells, marginal expression of pro-cathepsin G was detected in cell lysates. The pro and active forms of cathepsin G were markedly enhanced by Td92 treatment, and the active form was the predominant form in both cell lysates and culture supernatants. Active cathepsin G release into culture supernatants was detected as early as 30 min after Td92 stimulation. Treatment of cells with a cathepsin G inhibitor (Figure 5b, left panel) and cathepsin G knockdown (Figure 5b, right panel) decreased Td92-induced caspase-4 activation, while caspase-4 knockdown did not affect cathepsin G activity (Supplementary Figure 7), suggesting that cathepsin G activation acts upstream of caspase-4 activation. As Td92 interacts with integrin $\alpha 5\beta 1$ to induce caspase-1 activation in macrophages,²² we analyzed whether knockdown of integrin $\alpha 5\beta 1$ affected the cathepsin G activity induced by Td92. Cathepsin G activity was significantly inhibited in HGFs transfected with siRNA specific for integrin $\alpha 5\beta 1$ (Figure 5c). Td92 also induced cathepsin G mRNA expression (Figure 5d). Double immunofluorescence assays showed that Td92 treatment for as little as 30 min resulted in coaggregation of cathepsin G and caspase-4 (Figure 6a), which was inhibited by treatment with a cathepsin G inhibitor (Figure 6b, left panel) or knockdown of cathepsin G gene expression using siRNA (Figure 6b, right panel). Td-G, the N-terminal half of Td92 that induced caspase-1 activation in macrophages,²² also induced coaggregation of cathepsin G and caspase-4 (Figure 6a). Td-B, the C-terminal half of Td92, did not induce coaggregation (Supplementary Figure 8). We further confirmed the interaction between cathepsin G and caspase-4 of Td92-treated cell lysates by immunoprecipitation assay (Supplementary Figure 9). In non-treated cells or cells treated with Td-B, cathepsin G interacted with caspase-4 at a basal level. No interaction between cathepsin G and caspase-1 was detected in Td92-treated or non-treated cells. It is noteworthy that active cathepsin G bound only to pro-caspase-4 (50 kDa) in cell lysates. This result is consistent with the observation that caspase-4 is secreted directly upon activation, which explains why active caspase-4 was rarely detected in cell lysates. To determine whether the interaction of cathepsin G and caspase-4 was specific for Td92, we tested the response to LPS. Shi *et al.*¹³ reported that intracellular LPS bound directly to caspase-4, resulting in caspase-4 oligomerization and activation. In our experiments, *Escherichia coli* LPS was introduced into HGFs using a transfection reagent and caspase-4 activation was assessed in the presence of recombinant CD14 and LBP, which are required for LPS signaling. We examined two types of LPS from different strains: LPS B4 from *E. coli* O111:B4 and LPS B5 from *E. coli* O55:B5. LPS B4 is a TLR4 agonist, whereas LPS B5 is a TLR2 and TLR4 agonist. Regardless of the transfection reagent used, both forms of LPS induced caspase-4 activation. However, the LPS did not activate cathepsin G, suggesting differences in the caspase-4 activation

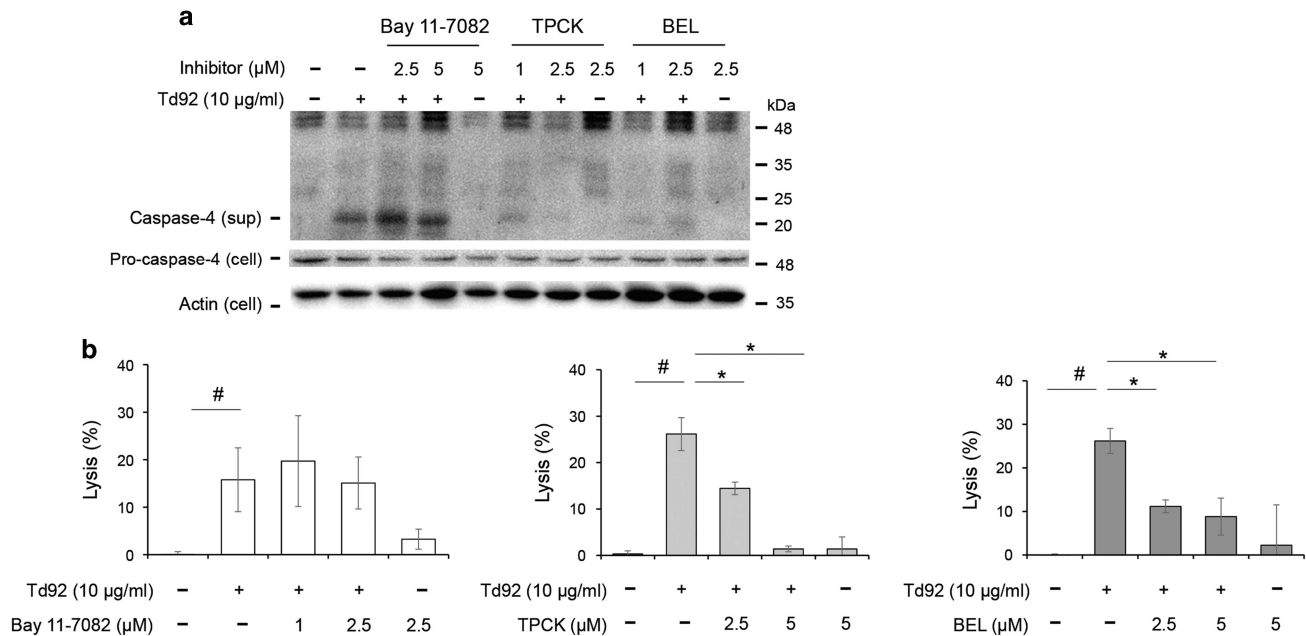


Figure 4 Serine protease inhibitors inhibit Td92-induced caspase-4 activation and cell death. (a and b) HGFs were pretreated with Bay 11-7082, TPCK or BEL at the indicated concentrations for 30 min before treatment with Td92 (10 μg/ml) for 6 h. Caspase-4 in the culture supernatants and pro-caspase-4 and actin in the cell lysates were detected by western blotting (a). LDH release in the culture supernatants was measured (b). Data are shown as the means ± S.D. of three independent experiments performed in triplicate. [#]*P* < 0.01 compared with non-treated controls and ^{*}*P* < 0.05 compared with Td92-stimulated cells

mechanism between Td92 and LPS (Supplementary Figure 10). Caspase-4 activation was also verified by adding active recombinant cathepsin G to non-treated HGF lysates (Figure 6c). Caspase-4 activation by cathepsin G was robust under acidic (pH 5) and neutral pH (pH 7.2) conditions. We also tested whether Td92 activated cathepsin G in HOK-16B cells, a human gingival epithelial cell line. As in HGFs, Td92 induced cathepsin G activation (Supplementary Figure 11a) and coaggregation of cathepsin G and caspase-4 in HOK-16B cells (Supplementary Figure 11b). Taken together, Td92 interaction with integrin α5β1 results in cathepsin G activation, which in turn causes caspase-4 activation by direct interaction.

Subcellular fractionation revealed that pro-cathepsin G was detected mostly in the cytosolic fraction in non-treated HGFs (Supplementary Figure 12a). In non-treated HGFs, active cathepsin G was detected both in the cytosolic and membrane fractions, although more active enzyme was detected in the cytosolic fraction than in the membrane fraction. After treatment of HGFs with Td92, active cathepsin G was detected in the cytosol, membrane fraction and the culture supernatants. These results suggest that cathepsin G in the cytosol is able to interact with caspase-4. Although the active form of cathepsin G in the cytosol fraction was detected at the same level in non-treated and Td92-treated cells, cathepsin G activity was significantly higher in Td92-treated cells (Figure 5a). Immunostaining of HGFs with anti-cathepsin G Ab and anti-LAMP-1 Ab did not show localization of cathepsin G in lysosomes, whereas cathepsin G was observed in the lysosomes of neutrophils (Supplementary Figure 12b). As Td92 induced cathepsin G mRNA expression (Figure 5d), our data indicate transcriptional activation and *de novo* synthesis

of cathepsin G by Td92, supporting the possible interaction of cathepsin G with caspase-4, which was also induced by Td92.

Td92-activated caspase-4 is associated with IL-1α secretion.

As caspase-1 activation and IL-1β secretion were not observed in Td92-treated HGFs, we analyzed IL-1α expression and secretion. Real-time RT-PCR revealed that Td92 induced IL-1α mRNA expression (Figure 7a). Td92-induced IL-1α expression was also confirmed at the protein level by ELISA and western blotting (Figure 7b). Interestingly, Td92-activated caspase-4 and IL-1α were detected in culture supernatants as early as 30 min after stimulation (Supplementary Figure 13a). Td92 activated the MAPK but not the NF-κB pathway in HGFs (Supplementary Figure 13b). MAPK inhibitors significantly inhibited Td92-induced IL-1α mRNA expression (Supplementary Figure 13c), but not IL-1α secretion or caspase-4 activation (Supplementary Figure 13d). Caspase-4 gene knockdown remarkably decreased the level of secreted IL-1α detected by western blotting (Figure 7c, left panel), whereas caspase-1 knockdown did not affect IL-1α secretion (Figure 7c, right panel). In addition, caspase-4 inhibitors decreased IL-1α secretion in Td92-treated HGFs (Supplementary Figure 13e), but not IL-8 secretion induced by Td92 (Supplementary Figure 13f). These results suggest that caspase-4 activation is specifically associated with IL-1α secretion. Treatment with a cathepsin G inhibitor (Figure 7d) and cathepsin G gene knockdown (Figure 7e) reduced Td92-induced IL-1α secretion, supporting our hypothesis that cathepsin G-dependent caspase-4 activation is a prerequisite for IL-1α secretion. However, gasdermin D knockdown by siRNA did not affect IL-1α secretion (data not shown).

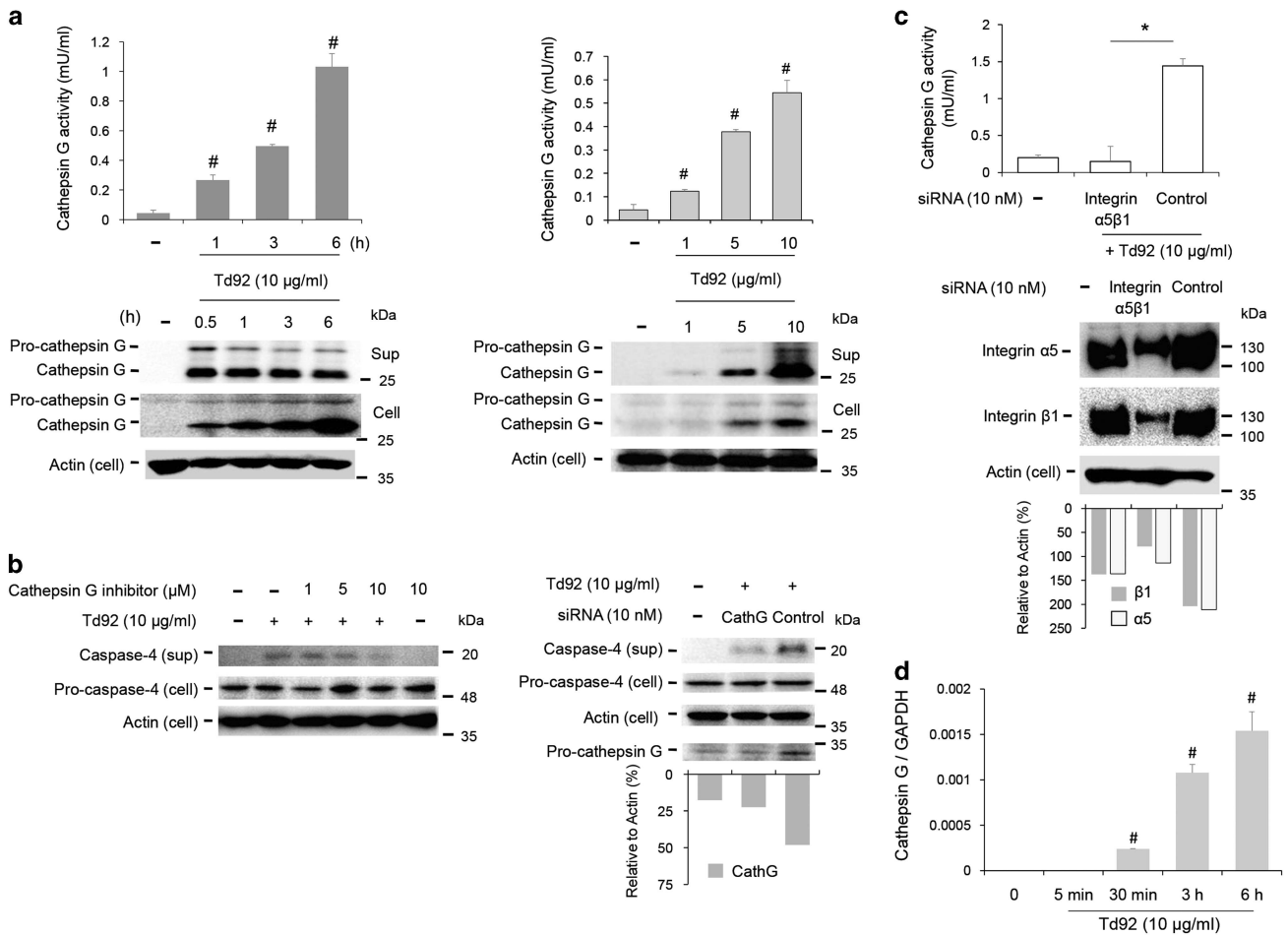


Figure 5 Td92-induced caspase-4 activation is associated with cathepsin G activity. (a) HGFs were treated with Td92 (1–10 µg/ml) for 0.5–6 h. Cathepsin G activity of HGFs was evaluated using a cathepsin G activity assay kit, and active cathepsin G and pro-cathepsin G in the supernatants and cell lysates were detected by western blotting. Data are shown as the means ± S.D. of three independent experiments performed in triplicate. [#]*P* < 0.01 compared with non-treated control. (b) HGFs were pretreated with cathepsin G inhibitor I at the indicated concentrations for 30 min or transfected with control siRNA or siRNA specific for cathepsin G (cathG) for 24 h before stimulation with Td92 (10 µg/ml) for 6 h. Caspase-4 in the culture supernatants and pro-caspase-4, pro-cathepsin G and actin in the cell lysates were detected by western blotting. (c) HGFs were transfected with control siRNA or siRNA specific for integrin α5 and β1 for 24 h. siRNA-transfected cells were treated with Td92 for 6 h and evaluated for cathepsin G activity. Transfection efficiency was confirmed by western blotting. Data are shown as the means ± S.D. of three independent experiments performed in triplicate. ^{*}*P* < 0.05 compared with control siRNA-transfected cells. Densitometric analysis of expression of cathepsin G (b) and integrin α5/β1 (c) relative to actin is shown. (d) HGFs were treated with Td92 for 5 min, 30 min, 3 and 6 h. The expression of cathepsin G mRNA was analyzed by real time RT-PCR. The data are shown as the means ± S.D. of three independent experiments. [#]*P* < 0.01 compared with non-treated control

In our previous study, we showed that Td92 activated caspase-1 via the NLRP3 inflammasome. However, NLRP3 knockdown did not affect cathepsin G activation, caspase-4 activation, or IL-1α secretion in HGFs (Supplementary Figure S14).

Discussion

In the present study, we demonstrated that Td92, a surface protein of the major periodontal pathogen *T. denticola*, induces caspase-4 activation and pyroptosis in HGFs via cathepsin G activation. Although Td92 induced both caspase-1 and caspase-4 in macrophages, Td92 activated only caspase-4 in HGFs. Therefore, Td92 and HGFs are an appropriate bacterial ligand and cell type, respectively, to study caspase-4 activation independent of caspase-1 activation. As Td92

homologs are found in different species of oral treponemes and *T. pallidum*,^{23,24} and the outer membranes of *Treponema* species are fragile,³² outer membrane proteins are released in the form of outer membrane vesicles into the environment. Thus, the local concentrations of surface proteins, including Td92, can be increased, and Td92 and its homologs can reach concentrations sufficient to induce cathepsin G activation.

Although we demonstrated that caspase-4 activation was independent of caspase-1 activation, other studies have reported a role for caspase-4 in caspase-1 activation. Caspase-4 has been shown to be required for caspase-1 activation via the NLRP3 inflammasome in keratinocytes in response to UVB irradiation.¹⁴ Caspase-4 is also required for caspase-1 activation in bone marrow-derived macrophages of caspase-4 transgenic mice stimulated with LPS or Pam3CSK4 in the absence of ATP, the signal required for

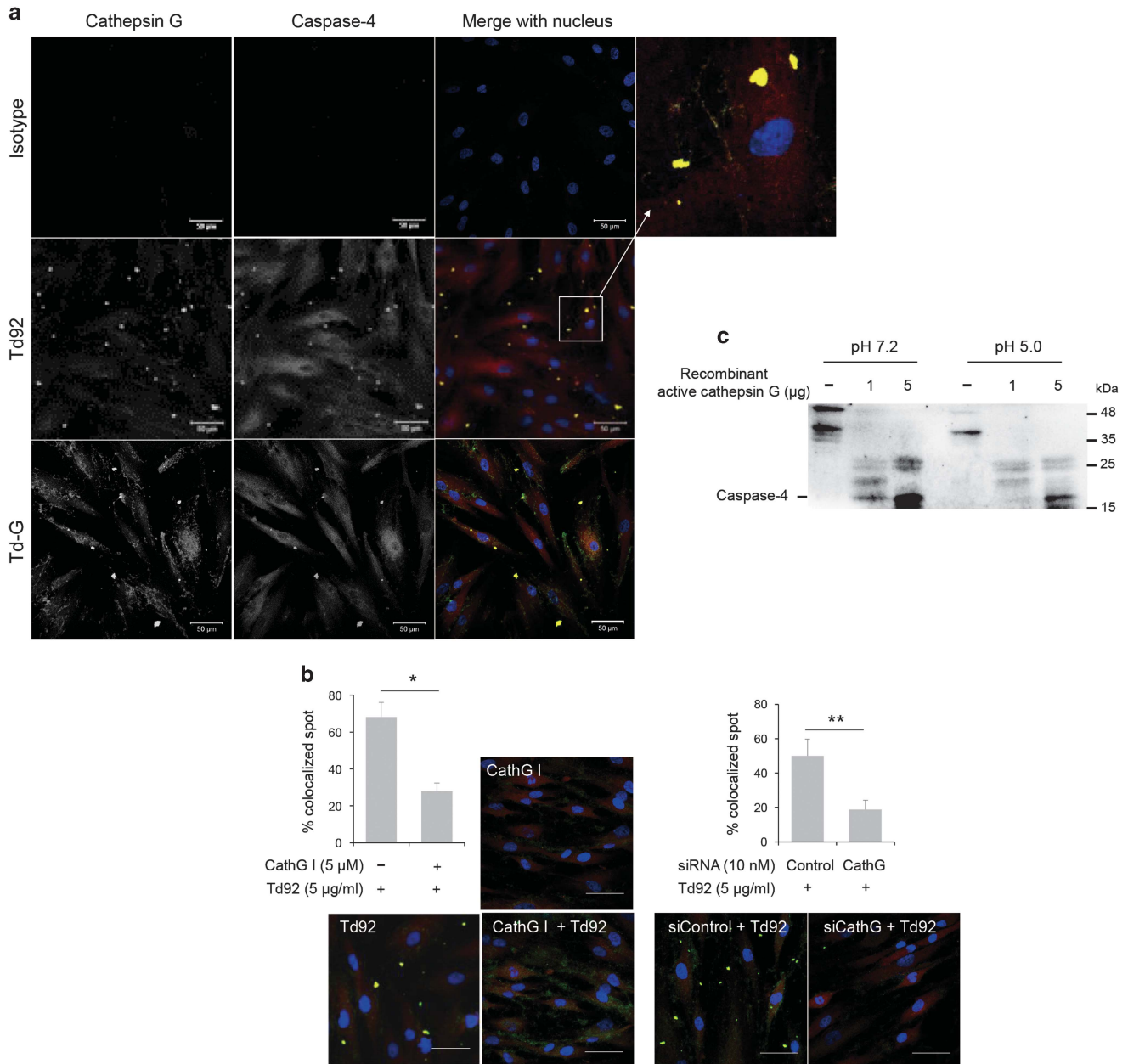


Figure 6 Caspase-4 interacts by cathepsin G by Td92 treatment. (a) HGFs were treated with Td92 (10 μ g/ml) or Td-G (5 μ g/ml) for 1 h. Stimulated cells were incubated with anti-cathepsin G antibody and anti-caspase-4 antibody followed by incubation with Cy3- and FITC-conjugated secondary antibodies, respectively. Cells were imaged by confocal laser scanning microscopy. Scale bars represent 50 μ m. (b) HGFs were pretreated with cathepsin G inhibitor I (CatG I) for 30 min or transfected with control siRNA or siRNA specific for cathepsin G for 24 h prior to stimulation with Td92 for 1 h. Images of 10 microscopic fields per well were taken at \times 200 magnification, and the percentage of coaggregates was calculated relative to total cells using NIH ImageJ software. At least 500 cells were counted for each experimental condition. Data are shown as the means \pm S. D. of three independent experiments. * P < 0.01 compared with Td92-stimulated cells. ** P < 0.01 compared with control siRNA-transfected cells. Scale bars represent 50 μ m. (c) HGF lysates (100 μ g of protein) were incubated with active recombinant cathepsin G at the indicated concentrations in pH 7.2 or pH 5.0 Tris-HCl buffer at 37 $^{\circ}$ C for 1 h. The resulting lysates were subjected to western blotting for the detection of caspase-4

inflammasome assembly and results in IL-1 β and IL-18 secretion.³³ Although various bacteria and their molecules activate caspase-1,³⁴ limited numbers of microbial ligands activate caspase-4. A recent study demonstrated that intracellular LPS interacts directly with the caspase activation and recruitment domain of caspase-4 and caspase-11, causing oligomerization and activation of these caspases

followed by pyroptosis.¹³ In our study, LPS induced caspase-4 activation in HGFs, but it did not induce cathepsin G, indicating that caspase-4 activation by Td92 is distinct from that by LPS.

Cathepsin G is found in the azurophilic granules of neutrophils and can be secreted or become membrane-associated upon activation. It has both physiological and

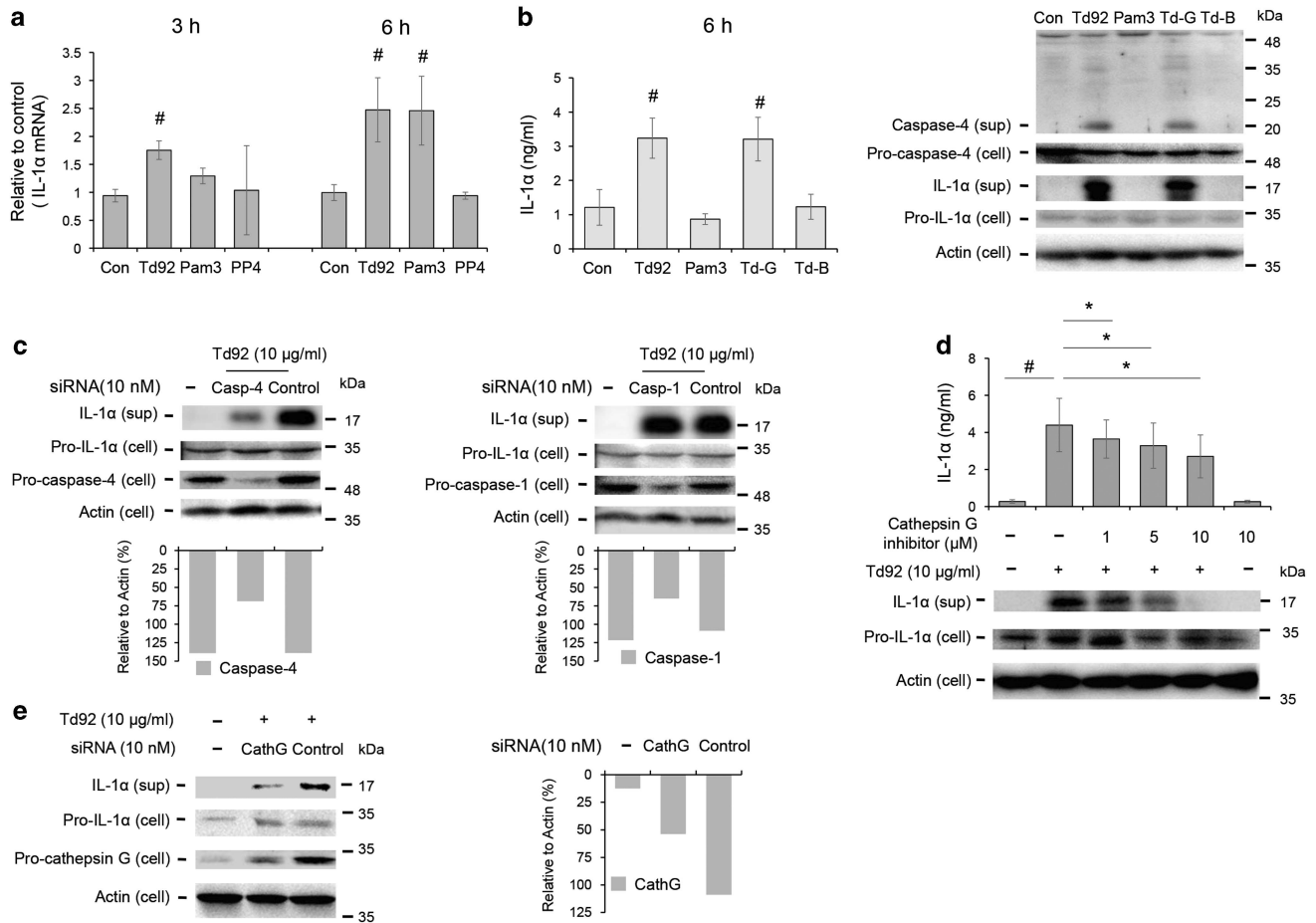


Figure 7 Td92 induces IL-1 α expression and secretion. (a and b) HGFs were treated with Td92 (10 μ g/ml), Pam3CSK4 (Pam3, 0.5 μ g/ml), PP4 (10 μ g/ml), Td-G (5 μ g/ml) or Td-B (5 μ g/ml) for 3–6 h. The expression of IL-1 α mRNA was analyzed by real time RT-PCR (a) and secreted IL-1 α was analyzed by ELISA (b, left panel) and western blotting (b, right panel). Data are shown as the means \pm S.D. of three independent experiments performed in triplicate. $^{\#}P < 0.01$ compared with non-treated controls. (c) HGFs were transfected with control siRNA, siRNA specific for caspase-4 (Casp-4) or caspase-1 (Casp-1) for 24 h. siRNA-transfected cells were treated with Td92 for 6 h. IL-1 α in the culture supernatants and pro-IL-1 α , pro-caspase-4, pro-caspase-1 and actin in the cell lysates were detected by western blotting. (d) HGFs were pretreated with cathepsin G inhibitor I at the indicated concentrations for 30 min before stimulation with Td92 (10 μ g/ml) for 6 h. IL-1 α level in the culture supernatants was analyzed by ELISA and western blotting. Data are shown as the means \pm S.D. of three independent experiments performed in triplicate. $^{\#}P < 0.01$ compared to non-treated controls and $^*P < 0.01$ compared to Td92-stimulated cells. (e) HGFs were transfected with control siRNA or siRNA specific for cathepsin G (cathG) for 24 h before stimulation with Td92 (10 μ g/ml) for 6 h. IL-1 α in the culture supernatants and pro-IL-1 α , pro-cathepsin G, and actin in the cell lysates were detected by western blotting. Densitometric analysis of expression of caspase-4 (c, left panel), caspase-1 (c, right panel) and cathepsin G (e) relative to actin is shown

pathological functions.¹⁹ Cathepsin G exerts antimicrobial activity by degrading pathogens in phagolysosomes or killing extracellular bacteria via proteolytic cleavage of the outer membrane.¹⁹ It degrades the extracellular matrix proteins fibronectin, collagen, proteoglycan and elastin, and activates matrix metalloproteinases, contributing to cell and tissue damage.^{20,35} Increased cathepsin G expression and activity are detected in the gingival tissue and crevicular fluid of periodontitis patients compared to those of healthy subjects.³⁶ *Mycobacterium tuberculosis* Rv3364c protein, a signal transduction operon component, inhibits cathepsin G activity by direct interaction with plasma membrane-associated cathepsin G in macrophages. This interaction results in the inhibition of caspase-1 activation and host cell death.³⁷ However, caspase-4 activation by cathepsin G, which is activated by a bacterial ligand, has not been reported.

Td92-activated caspase-4 was involved in IL-1 α processing and secretion in HGFs. Caspase-4-mediated IL-1 α secretion and cell death have also been observed in macrophages infected with Gram-negative pathogens.¹⁰ *L. pneumophila*, *Yersinia pseudotuberculosis* and *Salmonella typhimurium* induce caspase-4 activation, resulting in IL-1 α but not IL-1 β secretion. IL-1 α is implicated in host defense and inflammation, similar to IL-1 β .^{38–40} In contrast to gasdermin D-dependent secretion of IL-1 β processed by inflammatory caspases,^{4,6} IL-1 α secretion by Td92 in HGFs was not affected by gasdermin D knockdown, although it was decreased by caspase-4 knockdown and caspase-4 inhibitors.

Inflammatory cell death contributes to innate host defenses by eliminating invading bacteria during the early stages of infection and delayed cell death may facilitate bacterial

proliferation within cells.⁴¹ Continuous cell death results in the release of intracellular contents, with subsequent inflammation. The gingival tissues of periodontitis patients are exposed to multiple pathogen species, several of which invade epithelial cells and connective tissues composed of fibroblasts, macrophages and dendritic cells. Therefore, certain types of cell death benefit certain host cells, while damaging others. Gingival epithelial cell and fibroblast cell death from chronic inflammation can facilitate the penetration of periodontopathogens deep into tissues. Recent studies have demonstrated that periodontopathogens can induce pyroptosis via caspase-1 activation.^{22,42,43} As apoptosis shares several features in common with pyroptosis,⁴⁴ which has recently been studied in association with inflammasomes, types of cell death caused by periodontopathogens in periodontal tissue cells need to be investigated in greater detail to develop prognostic and diagnostic strategies. Pyroptosis, which is mediated via caspase-4 activation by periodontopathogens, is currently poorly understood.

In summary, we demonstrate that cathepsin G is directly engaged in caspase-4 activation in HGFs by Td92, a bacterial surface protein of a periodontal pathogen, without the involvement of caspase-1 and NLRP3. The interaction between Td92 and integrin $\alpha 5 \beta 1$ leads to cathepsin G activation. Td92-activated caspase-4 is responsible for pyroptosis and IL-1 α secretion. Elucidation of the mechanism by which Td92 causes cell death and an inflammatory response increases our understanding of the pathogenesis of *Treponema* infections, as Td92 homologs are present in diverse oral *Treponema* species, as well as *T. pallidum*.

Materials and Methods

Bacteria culture and Td92 preparation. *T. denticola* (ATCC 33521) was cultured in an anaerobic atmosphere (10% CO₂, 5% H₂ and 85% N₂) in new oral spirochrome broth (ATCC medium 1494). *T. denticola* surface protein Td92, the C-terminal half of Td92 (Td-B), the N-terminal half of Td92 (Td-G) and a partial peptide of *Treponema lecithinolyticum* MspTL(PP4) were prepared in recombinant six-histidine-tagged form by expression in *E. coli* and purification using Ni-NTA columns (Qiagen, Valencia, CA, USA) as described previously.²⁴ The absence of endotoxin in the recombinant protein preparations was verified using the Chinese hamster ovary/CD14/TLR4 cell line and polymyxin B (Sigma, St. Louis, MO, USA), as described previously.²² The endotoxin activity of the recombinant proteins was measured by the Limulus Amoebocyte Lysate (LAL) assay using a LAL Endochrome Kit (Charles River Endosafe, Wilmington, MA, USA) according to the manufacturer's protocol. The final preparations of recombinant Td92, Td-G, Td-B and PP4 contained 0.24, 0.21, 0.20 and 0.25 endotoxin units/ μ g of protein, respectively, corresponding to less than $\sim 1/30\,000$ of that of *E. coli* LPS of the same amount.

Chemicals and antibodies. Pam3CSK4, LPS-B4 ultrapure from *E. coli* O111:B4 and LPS-B5 ultrapure from *E. coli* 055:B5 were purchased from InvivoGen (San Diego, CA, USA). Staurosporine, the caspase-1 and -4 inhibitor Ac-YVAD-CHO, the caspase-4 inhibitor Ac-LEVD-CHO, SB203580 (a p38 MAPK inhibitor), SP600125 (a JNK inhibitor), PD98059 (an ERK inhibitor) and cathepsin G inhibitor I ([2-[3-[(1-benzoyl-piperidin-4-yl)-methyl-carbamoyl]-naphthalen-2-yl]-1-naphthalen-1-yl-2-oxoethyl]-phosphonic acid) were purchased from Calbiochem (San Diego, CA, USA). Thapsigargin, cytochalasin D, Bay 11-7082, BEL, TPCK and PI were purchased from Sigma. Annexin V was purchased from Invitrogen (Carlsbad, CA, USA). Rabbit polyclonal anti-caspase-1 Ab, rabbit monoclonal anti-LAMP-1 Ab (D2D11), rabbit monoclonal anti-phospho-SARK/JNK Ab (Thr183/Tyr185), rabbit monoclonal anti-phospho-p44/42 Ab (Thr202/Tyr204), rabbit polyclonal anti-phospho-p38 Ab, rabbit polyclonal anti-I κ B α Ab, rabbit polyclonal anti-integrin $\alpha 5$ Ab and rabbit polyclonal anti-integrin $\beta 1$ Ab were purchased from Cell Signaling Technology (Beverly, MA, USA). Recombinant cathepsin G, mouse monoclonal anti-

LAMP-1 Ab and mouse anti-Calcium Pump pan PMCA ATPase Ab (5F10) were purchased from Abcam (Cambridge, MA, USA). Goat polyclonal anti-caspase-4 Ab, mouse monoclonal anti-caspase-3 Ab, goat polyclonal anti-IL-1 β Ab, rabbit polyclonal anti-IL-1 α Ab and rabbit polyclonal anti-cathepsin G Ab were purchased from Santa Cruz Biotechnology (Santa Cruz, CA, USA). Anti-gasdermin D Ab was purchased from Proteintech (Rosemont, IL, USA). Mouse monoclonal anti-NLRP3 Ab (Cryo-2) was purchased from AdipoGen (San Diego, CA, USA). Mouse monoclonal anti-actin Ab was obtained from BD Biosciences (San Jose, CA, USA) and mouse anti-integrin $\alpha 5 \beta 1$ Ab from Chemicon (Temecula, CA, USA). Recombinant human CD14 and mouse anti-IFN β Ab were purchased from BioLegend (San Diego, CA, USA). Recombinant human LBP was purchased from R&D Systems (Minneapolis, MN, USA). Mouse IgG isotype control was purchased from eBioscience (San Diego, CA, USA), and rabbit and goat IgG isotypes were purchased from Southern Biotech (Birmingham, AL, USA).

Cell culture and stimulation. THP-1 cells (ATCC TIB-202), a human monocytic cell line, were cultured in RPMI 1640 medium supplemented with 10% fetal bovine serum (FBS), 100 U/ml penicillin and 100 μ g/ml streptomycin, and differentiated into macrophages by 0.5 μ M PMA treatment for 3 h. Human PBMC-derived monocytes were isolated using Ficoll-Paque PLUS (Amersham Biosciences, Piscataway, NJ, USA) and differentiated into macrophages in RPMI 1640 with 10% FBS for 6 days. To isolate neutrophils, human blood (10 ml) diluted in saline solution (0.9% NaCl) at a ratio of 1 : 1 was layered on 10 ml of Ficoll-Paque PLUS and then centrifuged at 400 \times g for 40 min at 20 °C. The cell pellet, which contained granulocytes and red blood cells, was subjected to hypotonic lysis of red blood cells three times, as described previously.⁴⁵ Human PBMCs were isolated by Ficoll-Paque density gradient centrifugation of whole blood. Cells were then cultured in RPMI 1640 medium supplemented with 10% FBS, 100 U/ml penicillin and 100 μ g/ml streptomycin for 6 days to induce their differentiation into macrophages. After adherent cells were detached using trypsin/EDTA (GIBCO, Invitrogen, Carlsbad, CA, USA), PBMC-derived macrophages were seeded into six-well plates (2×10^6 cells/well) and cultivated for 24 h. The Institutional Review Board of Seoul National University approved the collection of human blood (No. S-D20100008). HGFs were obtained from gingival tissue explants of periodontally healthy subjects under approval of the Institutional Review Board of Korean University Anam Hospital (No. AN10053-001). Primary cultured HGFs were cultured in DMEM supplemented with 10% FBS as described previously.⁴⁶ HOK-16B cells, an immortalized human epithelial cell line, were cultured in keratinocyte growth medium containing a supplementary growth factor bullet kit (KGM; Clonetics, San Diego, CA, USA).⁴⁷

THP-1 cells (2×10^6 cells/well in six-well plates), PBMC-derived macrophages (2×10^6 cells/well in six-well plates), HGFs (2×10^5 cells/well in six-well plates) and HOK-16B cells (5×10^5 cells/well in six-well plates) were treated with Td92, Td-G, Td-B, PP4 (unrelated recombinant protein), Pam3CSK4, thapsigargin or staurosporine at the indicated concentrations in serum-free medium for 1 to 24 h. To deliver LPS into the cytosol, LPS (1 μ g/ml) was pre-incubated with 1 μ M Lipofectamine (Invitrogen) for 20 min at room temperature before stimulation in medium containing 200 ng/ml of CD14 and 200 ng/ml of LBP. In the inhibition assay, cells were pretreated with the caspase-1 and -4 inhibitor Ac-YVAD-CHO, caspase-4 inhibitor Ac-LEVD-CHO, cytochalasin D, Bay 11-7082, BEL, TPCK, SB203580, SP600125, PD98059, cathepsin G inhibitor I, anti-integrin $\alpha 5 \beta 1$, anti-IFN β Ab or IgG isotype control at the indicated concentrations for 30 min or 1 h before stimulation.

Western blotting. Cells treated with different stimuli were washed with chilled PBS and lysed in 50 μ l modified RIPA buffer (10 mM Tris-HCl, pH 7.5, 150 mM NaCl, 1% Triton X-100, 50 mM NaF, 1 mM EDTA, 5 μ M Na₃VO₄, 1 mM phenylmethylsulfonyl fluoride (PMSF) and 1 \times protease inhibitor cocktail (Roche, Mannheim, Germany)). Lysates were clarified by centrifugation at 13 000 \times g for 45 min at 4 °C. The protein concentration was determined using a bicinchoninic acid protein assay kit. Cell lysates (100 μ g) and 10% trichloroacetic acid-precipitated supernatants were separated by SDS-PAGE (12% gel) and transferred to PVDF membranes. Membranes were probed with the following primary antibodies: anti-phospho-SARK/JNK (Thr183/Tyr185) Ab, anti-phospho-p44/42 (Thr202/Tyr204) Ab, anti-phospho-p38 Ab, anti-I κ B α Ab, anti-integrin $\alpha 5$ Ab, anti-integrin $\beta 1$ Ab, anti-caspase-4 Ab, anti-caspase-1 Ab, anti-caspase-3 Ab, anti-IL-1 β Ab, anti-IL-1 α Ab, anti-cathepsin G Ab, anti-gasdermin D Ab, anti-NLRP3 Ab (Cryo-2) and anti-actin Ab. Binding of the primary antibodies was detected using horseradish peroxidase-conjugated secondary antibodies (anti-rabbit, anti-goat and anti-mouse IgG, R&D Systems, Minneapolis, MN, USA) and ECL western blotting substrate (SUPEX, Dyne-Bio, Sungnam, Korea).

LDH assays. HGFs (2×10^4 cells/well in 96-well plates) were stimulated with Td92 at the indicated concentrations in the presence or absence of various inhibitors for 6 h. In some experiments, HGFs were transfected with siRNA for caspase-1, caspase-4, gasdermin D or control for 24 h before stimulation with Td92 for 6 h. LDH activity in the culture supernatants was measured using an LDH Cytotoxicity assay kit (BioVision, Palo Alto, CA, USA) according to the manufacturer's instructions. Cell death was calculated as the percentage of LDH release compared with maximal LDH release (100%) obtained by cell lysis with 1% Triton X-100.

Annexin V and PI staining. HGFs (2×10^5 cells/well in six-well plates) were stimulated with Td92 (10 μ g/ml) or staurosporine (1 μ g/ml) for 4 to 16 h after pretreatment with Ac-YVAD-CHO (50 μ M) or Ac-LEVD-CHO (50 μ M) for 30 min. Cells were washed with chilled PBS and stained with Annexin V (3 μ l) and PI (1 μ g/ml) in 100 μ l of Annexin V binding buffer (10 mM HEPES, 140 mM NaCl, 2.5 mM CaCl_2 , pH 7.4) for 15 min at room temperature. After adding 400 μ l of 1 \times Annexin V binding buffer, cells were analyzed by flow cytometry.

TUNEL assays. A TUNEL assay was performed to detect nuclear fragmentation. HGFs (5×10^4 cells/well in 24-well plates) were cultured on cover glasses and pretreated with Ac-YVAD-CHO (50 μ M) or Ac-LEVD-CHO (50 μ M) for 30 min before stimulation with Td92 (10 μ g/ml) for 16 h. To generate artificial DNA fragmentation, cells in several experiments were treated with DNase I (Roche; 10 units/ml) and then subjected to TUNEL assays according to the manufacturer's protocol (Promega, Madison, WI, USA). Cells were observed by confocal laser scanning microscopy (LSM 700, Carl Zeiss, Jena, Germany). Images of 10 microscopic fields per well were taken at $\times 200$ magnification and the percentage of TUNEL-positive cells was calculated using NIH ImageJ software developed at the National Institutes of Health (<http://rsbweb.nih.gov/ij/>). At least 500 cells were counted for each experimental condition.

Reverse-transcription quantitative PCR. Total RNA was prepared from HGFs stimulated with Td92 in the presence or absence of various inhibitors using an easy-BLUE total extraction kit (iNtRON Biotechnology, Sungnam, Korea) and cDNA was synthesized using an M-MLV Reverse Transcriptase kit (Promega) according to the manufacturer's protocol. For qPCR, cDNA (1 μ l) was mixed with 10 μ l of SYBR Premix Ex Taq (Takara Bio Inc., Kyoto, Japan) and primer pairs (4 pmol each) in a 20 μ l reaction volume, followed by 40 PCR cycles of denaturation at 95 $^\circ\text{C}$ for 15 s, annealing at 60 $^\circ\text{C}$ for 15 s and extension at 72 $^\circ\text{C}$ for 33 s, using an ABI PRISM 7500 Fast Real-Time PCR System (Applied Biosystems, Foster City, CA, USA). Glyceraldehyde dehydrogenase (GAPDH) was used as a reference house-keeping gene to normalize expression levels and to quantify changes in gene expression between non-treated controls and stimulated cells. Primer sequences were as follows: 5'-GCT GAA GGA GAT GCC TGA GAT-3' and 5'-AGA CCT ACG CCT GGT TTT CC-3' for IL-1 α ; 5'-ACT CTG AGG CTC TTT CCA ACG -3' and 5'-TTC TGT GGT TGC CTT CTG CC-3' for caspase-4; 5'-GAC TAT TGT TGA GAA CCT CCT-3' and 5'-TCG GAG GTA ACC TGT AAG TC-3' for IFN- β ; 5'-GTC TAA GGC ACT GAG CGT ATC A-3' and 5'-GGA TCA GTC TGC TTT CAG GTG TG-3' for CHOP; 5'-CCA ACG CCA AGC AAC CAA AGA CG-3' and 5'-CCA CCC AGG TCA AAC ACC AGG ATG-3' for GRP78; 5'-GAG TCA GAC GGA ATC GAA ACG-3' and 5'-CGG AGT GTA TCT GTT CCC CTC-3' for cathepsin G; 5'-GTC GCC AGC CGA GCC-3' and 5'-TGA AGG GGT CAT TGA TGG CA-3' for GAPDH.

RNA interference assays. siRNA duplexes were designed with the Invitrogen Block-iT RNAi Designer program. The gene accession numbers are NM_001223.3 (CASP1), NM_001225.3 (CASP4), NM_002205 (ITGA5), NM_033668 (ITGB1), NM_001911.2 (CTSG), NM_024736 (GSDMD) and NM_001079821 (NLRP3), and the sequences of the duplexes were as follows: sense: 5'-GGA AGU GAA GAG AUC CUU CUG UAA A-3' and antisense: 5'-UUU ACA GAA GGA UCU CUU CAC UUC C-3' for the siCaspase-1 duplex; sense: 5'-GGG CAA AGA UUU CCU CAC UGG UGU U-3' and antisense: 5'-AAC ACC AGU GAG GAA AUC UUU GCC C-3' for the siCaspase-4 duplex; sense: 5'-UGG CCA UGA GUU UGG CCG AUU U-3' and anti-sense: 5'-AAA UCG GCC AAA CUC AUC AUG GCC A-3' for the siIntegrin $\alpha 5$ duplex; sense: 5'-UCA AAU UGA ACC UCA UCU CCA AUG G-3' and anti-sense: 5'-CCA UUG GAG AUG AGG UUC AAU UUG A-3' for the siIntegrin $\beta 1$ duplex; sense: 5'-GAG CCA UCC GCC ACC CUC AAU AUA A-3' and anti-sense 5'-UUA UAU UGA GGG UGG CGG AUG GCU C-3' for the siCathepsin G duplex;

sense: 5'-CGG AAC UCG CUA UCC CUG UUG UCU A-3' and anti-sense: 5'-UAG ACA GGG AUA GCG AGU UCC G-3' for the siGasdermin D duplex; and sense: 5'-ACC GCG GUG UAC GUC UUC CUU U-3' and anti-sense: 5'-AAA GGA AGA CGU ACA CCG CGG U-3' for the siNLRP3 duplex. Each siRNA and stealth RNAi-negative control duplex (Invitrogen) was resuspended at a final concentration of 20 μ M. Lipofectamine RNAiMAX (Invitrogen) diluted in 250 μ l of serum-free media without antibiotics was mixed with an equal volume of diluted siRNA (10 or 30 nM). HGFs (2×10^5 cells/well in six-well plates) in culture medium containing 10% FBS without antibiotics were transfected with the RNAiMAX/siRNA mixtures. After a 24 h incubation, cells were treated with Td92 as described above.

Cathepsin G activity assay. HGFs (8×10^5 cells/well in 100 Φ dishes) were stimulated with different doses of Td92 for different incubation times. In some experiments, cells were transfected with siRNA for integrin $\alpha 5$, integrin $\beta 1$, caspase-4 or control siRNA and then stimulated with Td92. After cell lysis, cathepsin G activity was measured using a cathepsin G activity assay kit according to the manufacturer's instructions (BioVision). Cathepsin G activity was recorded as mU/ml and one unit was defined as the amount of cathepsin G that hydrolyzes the pNA (4-Nitroaniline)-based peptide substrate (MeOSuc-Ala-Ala-Pro-Met-pNA) to produce 1.0 μ mol of 4-nitroaniline per minute at 37 $^\circ\text{C}$.

Confocal microscopy. HGFs (6×10^4 cells/well), HOK-16B (1×10^5 cells/well) and neutrophils (2×10^6 cells/reaction) on cover glasses in 24-well plates were stimulated as indicated. In several experiments, HGFs (6×10^4 cells/well at 24-well plates) were transfected with siCathepsin G or siControl for 24 h or preincubated with cathepsin G inhibitor I for 30 min. Stimulated cells were washed twice with PBS, fixed with 4% paraformaldehyde and blocked with 1% rabbit serum and 1% donkey serum in PBS (blocking solution). Cells were then incubated with rabbit anti-cathepsin G Ab, goat anti-caspase-4 Ab, mouse anti-LAMP-1 Ab, isotype rabbit IgG, isotype goat IgG or isotype mouse IgG followed by incubation with Cy3- and FITC-conjugated secondary antibodies (Jackson ImmunoResearch Laboratories, Baltimore, PA, USA) in blocking solution. Nuclei were stained with Hoechst 33342. Cells were observed under a confocal laser scanning microscope (LSM 700, Carl Zeiss). Images of 10 microscopic fields per well were taken at $\times 200$ magnification and the percentage of colocalized spots relative to total cells was calculated using NIH ImageJ software. At least 500 cells were counted for each experimental condition.

Immunoprecipitation assays. HGFs (8×10^5 cells/ 100 Φ dishes) were lysed with prechilled lysis buffer (25 mM HEPES, pH 7.5, 150 mM NaCl, 1% IGEPAL CA-630, 0.25% Na-deoxycholate, 10% glycerol, 1 \times protease inhibitor cocktail). After preclearing lysates with Protein G-agarose, the lysates were incubated with the indicated specific antibodies (3 μ g) or isotype IgG against each antibody at 4 $^\circ\text{C}$ overnight. Lysates were then incubated with 20 μ g of Protein G agarose (Chemicon) at 4 $^\circ\text{C}$ for 4 h. The reacted agarose was washed five times with lysis buffer, boiled in 2 \times SDS sample buffer and used for SDS-PAGE, followed by western blotting with the indicated antibodies.

Caspase-4 activation by recombinant active cathepsin G. HGFs (8×10^5 cells/100 Φ dishes) were lysed in 25 mM Tris-HCl buffer (pH 7.2 or pH 5.0) by sonication. The lysates (100 μ g) and recombinant active cathepsin G were co-incubated in 25 mM Tris-HCl buffer (pH 7.2 or pH 5.0) at 37 $^\circ\text{C}$ for 1 h. The reacted lysates were subjected to western blotting with caspase-4 antibody.

Cell fractionation. HGFs (8×10^5 cells/100 Φ dishes) were stimulated with Td92 for 1 h and the cells and supernatants were separately collected. After washing the cells with chilled extraction buffer (210 mM mannitol, 70 mM sucrose, 1 mM EDTA and 20 mM Hepes, pH 7.5) supplemented with 100 mM PMSF and 1 \times protease inhibitor cocktail (Roche), cells were disrupted by passage through a G27 needle until approximately 50% of the cells were positive for trypan blue. The total extracts were centrifuged at 1000 $\times g$ for 5 min at 4 $^\circ\text{C}$. The supernatants were collected and centrifuged at 20 800 $\times g$ for 1 h at 4 $^\circ\text{C}$. The upper cleared phase (cytosolic fraction) was collected and the pellet (membrane fraction) was lysed in lysis buffer as described in the procedure for western blotting. The cytosolic fraction, membrane fraction, and culture supernatants were analyzed by western blotting with the indicated antibodies. PMCA-1 was used as a control for the membrane fraction and actin as a control for the cytosolic fraction.

ELISA assay. Culture supernatants of HGFs treated with Td92, Pam3CSK4, Td-G or Td-B in the presence or absence of inhibitors were assayed to determine IL-1 α or IL-8 levels using ELISA kits from R&D Systems.

Statistical analysis. Statistically significant differences between experiments were analyzed using an unpaired, one-tailed Student's *t*-test. Data are shown as the means \pm S.D. A *P*-value < 0.05 was considered statistically significant.

Conflict of Interest

The authors declare no conflict of interest.

Acknowledgements. This study was supported by grants from the Basic Science Research Program of the National Research Foundation of Korea funded by the Ministry of Science, ICT and Future Planning (NRF-2015R1A2A2A01002598).

- Martinon F, Tschopp J. Inflammatory caspases and inflammasomes: master switches of inflammation. *Cell Death Differ* 2007; **14**: 10–22.
- Schroder K, Tschopp J. The inflammasomes. *Cell* 2010; **140**: 821–832.
- Bergsbaken T, Fink SL, Cookson BT. Pyroptosis: host cell death and inflammation. *Nat Rev Microbiol* 2009; **7**: 99–109.
- Kayagaki N, Stowe IB, Lee BL, O'Rourke K, Anderson K, Warming S et al. Caspase-1 cleaves gasdermin D for non-canonical inflammasome signalling. *Nature* 2015; **526**: 666–671.
- Ding J, Wang K, Liu W, She Y, Sun Q, Shi J et al. Pore-forming activity and structural autoinhibition of the gasdermin family. *Nature* 2016; **535**: 111–116.
- Shi J, Zhao Y, Wang K, Shi X, Wang Y, Huang H et al. Cleavage of GSDMD by inflammatory caspases determines pyroptotic cell death. *Nature* 2015; **526**: 660–665.
- Hitomi J, Katayama T, Eguchi Y, Kudo T, Taniguchi M, Koyama Y et al. Involvement of caspase-4 in endoplasmic reticulum stress-induced apoptosis and A β -induced cell death. *J Cell Biol* 2004; **165**: 347–356.
- Pelletier N, Casamayor-Palleja M, De Luca K, Mondiere P, Saltel F, Jurdic P et al. The endoplasmic reticulum is a key component of the plasma cell death pathway. *J Immunol* 2006; **176**: 1340–1347.
- Li C, Wei J, Li Y, He X, Zhou Q, Yan J et al. Transmembrane protein 214 (TMEM214) mediates endoplasmic reticulum stress-induced caspase-4 enzyme activation and apoptosis. *J Biol Chem* 2013; **288**: 17908–17917.
- Casson CN, Yu J, Reyes VM, Tschuk FO, Yadav A, Copenhaver AM et al. Human caspase-4 mediates noncanonical inflammasome activation against gram-negative bacterial pathogens. *Proc Natl Acad Sci USA* 2015; **112**: 6688–6693.
- Kayagaki N, Warming S, Lamkanfi M, Vande Walle L, Louie S, Dong J et al. Non-canonical inflammasome activation targets caspase-11. *Nature* 2011; **479**: 117–121.
- Knodler LA, Crowley SM, Sham HP, Yang H, Wrande M, Ma C et al. Noncanonical inflammasome activation of caspase-4/caspase-11 mediates epithelial defenses against enteric bacterial pathogens. *Cell Host Microbe* 2014; **16**: 249–256.
- Shi J, Zhao Y, Wang Y, Gao W, Ding J, Li P et al. Inflammatory caspases are innate immune receptors for intracellular LPS. *Nature* 2014; **514**: 187–192.
- Sollberger G, Strittmatter GE, Kistowska M, French LE, Beer HD. Caspase-4 is required for activation of inflammasomes. *J Immunol* 2012; **188**: 1992–2000.
- Grimstad O, Husebye H, Espevik T. TLR3 mediates release of IL-1 β and cell death in keratinocytes in a caspase-4 dependent manner. *J Dermatol Sci* 2013; **72**: 45–53.
- Kobayashi T, Ogawa M, Sanada T, Mimuro H, Kim M, Ashida H et al. The Shigella OspC3 effector inhibits caspase-4, antagonizes inflammatory cell death, and promotes epithelial infection. *Cell Host Microbe* 2013; **13**: 570–583.
- Salvesen G, Farley D, Shuman J, Przybyla A, Reilly C, Travis J. Molecular cloning of human cathepsin G: structural similarity to mast cell and cytotoxic T lymphocyte proteinases. *Biochemistry* 1987; **26**: 2289–2293.
- Kosikowska P, Lesner A. Inhibitors of cathepsin G: a patent review. *Expert Opin Ther Pat* 2013; **23**: 1611–1624.
- Pham CT. Neutrophil serine proteases: specific regulators of inflammation. *Nat Rev Immunol* 2006; **6**: 541–550.
- Son ED, Kim H, Choi H, Lee SH, Lee JY, Kim S et al. Cathepsin G increases MMP expression in normal human fibroblasts through fibronectin fragmentation, and induces the conversion of proMMP-1 to active MMP-1. *J Dermatol Sci* 2009; **53**: 150–152.
- Tribble GD, Lamont RJ. Bacterial invasion of epithelial cells and spreading in periodontal tissue. *Periodontol* 2000 2010; **52**: 68–83.
- Jun HK, Lee SH, Lee HR, Choi BK. Integrin $\alpha 5 \beta 1$ activates the NLRP3 inflammasome by direct interaction with a bacterial surface protein. *Immunity* 2012; **36**: 755–768.
- Cameron CE, Lukehart SA, Castro C, Molini B, Godornes C, Van Voorhis WC. Opsonic potential, protective capacity, and sequence conservation of the *Treponema pallidum* subspecies pallidum Tp92. *J Infect Dis* 2000; **181**: 1401–1413.
- Jun HK, Kang YM, Lee HR, Lee SH, Choi BK. Highly conserved surface proteins of oral spirochetes as adhesins and potent inducers of proinflammatory and osteoclastogenic factors. *Infect Immun* 2008; **76**: 2428–2438.
- Khare S, Dorfleutner A, Bryan NB, Yun C, Radian AD, de Almeida L et al. An NLRP7-containing inflammasome mediates recognition of microbial lipopeptides in human macrophages. *Immunity* 2012; **36**: 464–476.
- Broz P, Monack DM. Noncanonical inflammasomes: caspase-11 activation and effector mechanisms. *PLoS Pathog* 2013; **9**: e1003144.
- Bian ZM, Elnar SG, Elnar VM. Dual involvement of caspase-4 in inflammatory and ER stress-induced apoptotic responses in human retinal pigment epithelial cells. *Invest Ophthalmol Vis Sci* 2009; **50**: 6006–6014.
- Liu X, Zhang Z, Ruan J, Pan Y, Magupalli VG, Wu H et al. Inflammasome-activated gasdermin D causes pyroptosis by forming membrane pores. *Nature* 2016; **535**: 153–158.
- Franchi L, Chen G, Marina-Garcia N, Abe A, Qu Y, Bao S et al. Calcium-independent phospholipase A2 β is dispensable in inflammasome activation and its inhibition by bromoenol lactone. *J Innate Immun* 2009; **1**: 607–617.
- Zhou Q, Salvesen G. Activation of pro-caspase-7 by serine proteases includes a non-canonical specificity. *Biochem J* 1997; **324**: 361–364.
- Sabri A, Alcott SG, Elouardighi H, Pak E, Derian C, Andrade-Gordon P et al. Neutrophil cathepsin G promotes detachment-induced cardiomyocyte apoptosis via a protease-activated receptor-independent mechanism. *J Biol Chem* 2003; **278**: 23944–23954.
- Caimano MJ, Bourell KW, Bannister TD, Cox DL, Radolf JD. The *Treponema denticola* major sheath protein is predominantly periplasmic and has only limited surface exposure. *Infect Immun* 1999; **67**: 4072–4083.
- Kajiwara Y, Schiff T, Voloudakis G, Gama Sosa MA, Elder G, Bozdagi O et al. A critical role for human caspase-4 in endotoxin sensitivity. *J Immunol* 2014; **193**: 335–343.
- Franchi L, Muñoz-Planillo R, Núñez G. Sensing and reacting to microbes through the inflammasomes. *Nat Immunol* 2012; **13**: 325–332.
- Beklen A, Tüter G, Sorsa T, Hanemaaijer R, Virtanen I, Tervahartiala T et al. Gingival tissue and crevicular fluid co-operation in adult periodontitis. *J Dent Res* 2006; **85**: 59–63.
- Tervahartiala T, Konttinen YT, Ingman T, Häyrynen-Immonen R, Ding Y, Sorsa T. Cathepsin G in gingival tissue and crevicular fluid in adult periodontitis. *J Clin Periodontol* 1996; **23**: 68–75.
- Danelishvili L, Everman JL, McNamara MJ, Bermudez LE. Inhibition of the plasma-membrane-associated serine protease cathepsin G by *Mycobacterium tuberculosis* Rv3364c suppresses caspase-1 and pyroptosis in macrophages. *Front Microbiol* 2012; **2**: 281.
- Di Paolo NC, Miao EA, Iwakura Y, Murali-Krishna K, Aderem A, Flavell RA et al. Virus binding to a plasma membrane receptor triggers interleukin-1 α -mediated proinflammatory macrophage response in vivo. *Immunity* 2009; **31**: 110–121.
- Joosten LA, Van De Veerdonk FL, Vonk AG, Boerman OC, Keuter M, Fantuzzi G et al. Differential susceptibility to lethal endotoxaemia in mice deficient in IL-1 α IL-1 β or IL-1 receptor type I. *APMIS* 2010; **118**: 1000–1007.
- Vonk AG, Netea MG, van Krieken JH, Iwakura Y, van der Meer JW, Kullberg BJ. Endogenous interleukin (IL)-1 α and IL-1 β are crucial for host defense against disseminated candidiasis. *J Infect Dis* 2006; **193**: 1419–1426.
- Miao EA, Rajan JV, Aderem A. Caspase-1-induced pyroptotic cell death. *Immunol Rev* 2011; **243**: 206–214.
- Taxman DJ, Swanson KV, Brogdie PM, Wen H, Holley-Guthrie E, Huang MT et al. Porphyromonas gingivalis mediates inflammasome repression in polymicrobial cultures through a novel mechanism involving reduced endocytosis. *J Biol Chem* 2012; **287**: 32791–32799.
- Park E, Na HS, Song YR, Shin SY, Kim YM, Chung J. Activation of NLRP3 and AIM2 inflammasomes by Porphyromonas gingivalis infection. *Infect Immun* 2014; **82**: 112–123.
- Duprez L, Wirawan E, Vanden Berghe T, Vandenabeele P. Major cell death pathways at a glance. *Microbes Infect* 2009; **11**: 1050–1062.
- Nauseef WM Isolation of human neutrophils from venous blood: Quinn MT, DeLeo FReds *Neutrophil Methods and Protocols* 2nd edn Humana Press Inc: Totowa, NJ, USA, 2014 pp 13–18.
- Choi BK, Jung JH, Suh HY, Yoo YJ, Cho KS, Chai JK et al. Activation of matrix metalloproteinase-2 by a novel oral spirochetal species *Treponema lecithinolyticum*. *J Periodontol* 2001; **72**: 1594–1600.
- Park NH, Min BM, Li SL, Huang MZ, Cherick HM, Doniger J. immortalization of normal human oral keratinocytes with type 16 human papillomavirus. *Carcinogenesis* 1991; **12**: 1627–1631.

Supplementary Information accompanies this paper on Cell Death and Differentiation website (<http://www.nature.com/cdd>)